Subsonic Jet Noise Prediction in Near and Far Field with Optimized Wave-Packet Approach

Giorgio Palma, Stefano Meloni, Roberto Camussi, Umberto Iemma, Christophe Bogey

Subsonic Jet Noise Prediction in Near and Far Field with Optimized Wave-Packet Approach

Giorgio Palma *
CNR-INM, National Research Council-Institute of Marine Engineering, 00128 Roma, Italy

Stefano Meloni,†
University of Tuscia, 01100 Viterbo, VT, Italy

Roberto Camussi,‡ and Umberto Iemma,§
Roma Tre University, 00146 Roma, RM, Italy

Christophe Bogey ¶
Laboratoire de Mécanique des Fluides et d'Acoustique, LMFA, UMR 5509, 69130 Ecully, France

In this study, the parameters of a wave-packet model for subsonic jet noise prediction are systematically optimized by leveraging near- and far-field data obtained from the large eddy simulation (LES) of a free jet at a Mach number of 0.9 across various radial distances. The utilization of near-field information is justified by the observation that the scattering surfaces are typically situated within a few nozzle diameters from the jet axis in the radial direction both in current and innovative aircraft configurations. The far-field information is used to guarantee the correct subdivision between the wave-packet radiating noise and the hydrodynamic components. The results show a notable agreement between the LES data and the wave-packet solutions, consistent with findings documented in the existing literature. This agreement underscores the validity and applicability of the implemented methodology, offering an effective method for obtaining an equivalent jet noise acoustic source, easily implementable in acoustic scattering codes, accounting for the directional behavior of jet noise.

*Research Scientist, INM Rome, Via di Vallerano, 139, 00128 Roma. Corresponding Author, giorgio.palma@cnr.it, AIAA Member

†Assistant Professor, Department of Economics, Engineering, Society and Business Organization, Corresponding Author, stefano.meloni@unitus.it, AIAA Member

‡Full Professor, Department of Civil, Computer Science and Aeronautical Engineering, Via Vito Volterra, 62, 00146 Roma, roberto.camussi@uniroma3.it, Associate Fellow AIAA

§Full Professor, Department of Civil, Computer Science and Aeronautical Engineering, Via Vito Volterra, 62, 00146 Roma, umberto.iemma@uniroma3.it

¶CNRS Research Scientist; CNRS, Ecole Centrale de Lyon, Université Claude Bernard Lyon I, christophe.bogey@ec-lyon.fr. Associate Fellow AIAA.

Presented as Paper AIAA 2023-3832 at the 2023 AIAA Aviation and Aeronautics Forum and Exposition, San Diego, California, USA, June 12-16, 2023;

Nomenclature

x, r, θ	=	cylindrical coordinates
R	=	polar distance from the center point of nozzle exit section
c_∞	=	speed of sound of the unperturbed flow
D	=	nozzle exhaust diameter
p	=	pressure
f	=	frequency
ω	=	$2\pi f$ angular frequency in radians
k	=	ω/c_∞ acoustic wave–number
Re_D	=	$\rho U D/\mu$ nozzle exhaust Reynolds number
He_l	=	kl Helmholtz number with characteristic length l
St	=	fD/U Strouhal number
U_j	=	nozzle exhaust jet velocity
M	=	U_j/c_∞ jet Mach number
δ_{BL}	=	nozzle exhaust boundary layer
J	=	objective function
$\mathbf{q}$	=	parameters vector
$\mathbf{v}$	=	design variables vector
TI	=	Turbulence Intensity
SPL	=	Sound Pressure Level

I. Introduction

Aviation noise has been widely identified as a driver of several negative stress-mediated health effects, from sleep disorders to cardiovascular issues [1, 2], which incidence is increased in the exposed population. The operation and expansion of airports are nowadays limited by strict regulations aiming at controlling and limiting the exposure of the surrounding community to aircraft noise and the number of people affected by it. Forecasts of the international regulation authorities indicate that this situation is the most likely scenario in the future, with increasing air traffic at least for most regions of the world [3].

The research on noise reduction devices is nowadays very active in all the aircraft areas, involving relatively mature technologies for quieter high lift devices [4], chevrons for jet exhaust [5, 6], the evolution of acoustic liners [7–12] for turbofans ducts, and also more innovative treatments with lower Technology Readiness Level [13]. Projecting the research to the mid- and long-term future, groundbreaking solutions are also being developed, aiming at overcoming the

saturation trend in noise reduction that characterizes mature technologies. Innovative configurations such as Blended and Hybrid Wing Body (BWB and HWB) aircraft are probably the most promising alternative to the well-known tube-and-wing configuration in terms of aerodynamic efficiency and community noise reduction [14–17]. The most popular interpretation of these innovative configurations involves the upper installation of the propulsion system on top of the large center body surface, offering interesting acoustic shielding capability to be exploited for engine-related community noise reduction [13, 18, 19]. The propulsion-airframe acoustic interaction is an aspect of growing research interest for future aircraft and should be accounted for since the beginning of the design process, with particular attention to jet noise.

Jet noise has always been a dominant noise source for turbojets and turbofans especially during take-off operations. Over the past 50 years, subsonic jet noise has garnered significant attention and has remained a focal point in the design of modern and future civil aircraft. This emphasis stems from the importance of addressing and minimizing the noise impact associated with these aircraft.

However, the simulation of the scattering and shielding from large surfaces in the audible range of frequencies can be computationally very expensive, requiring accurate solutions up to extremely high Helmholtz number $He = kl$ (where k is the wave-number for the propagating acoustic disturbance and l is the characteristic length of the scattering object). The resources required for direct simulation with high-fidelity CFD or CAA methods make them unfeasible for extensive usage in the conceptual design phase and design optimization processes. There is hence a strong need for low- and mid-fidelity models and solvers able to catch the fundamental feature of installed jet noise, avoiding the solution of the complete set of equations holding the dynamic of the complex fluid structures involved.

In this framework, since the publication of Lighthill [20] many researchers investigated jet-induced pressure fluctuations both in the near field and in the far field in the attempt to develop models able to predict as accurately as possible the emitted noise. Nevertheless, despite many published papers. jet noise remains a beautiful puzzle with intricate pieces due to the complex physics.

The discovery of coherent structures in jets changed the perspective of jet noise and provided a basis for introducing the wave-packet approach [21]. As suggested by Huang and Papamoschou [22], the wave-packet is an amplitude-modulated traveling pressure wave. Several authors have widely used this approach to predict and model the jet noise source from far-field measurements having parameters such as envelope amplitude, wavelength, position, and convection velocity. The wave-packet model has been widely used as a low-order model for the jet noise source both in subsonic and supersonic regimes [23, 24]. In Huang and Papamoschou [22], a virtual cylindrical surface hosting the wave-packet is assumed to surround the jet region and radiate the pressure perturbations. The parameters such as the envelope amplitude, wavelength, position, and convection velocity were typically estimated from far-field measurements, optimizing their values and maximizing the agreement with experimental data on a training set [25–27].

Recently, Palma *et. al.* [28] followed the approach introduced by Papamoschou [22, 25–27], calibrating the

model parameters on near-field LES data of a high-speed subsonic isothermal jet. The mentioned paper presents a multi-Strouhal number (St) analysis optimizing the wave-packet source model separately for each value in the set St = 0.25, 0.5, 0.75 and 1 and using pressure data from the numerical database for the dominant axisymmetric 0^{th} azimuthal mode. It has been shown that optimizing the model parameters with pressure data at multiple distances in the near field provides a noise source that also preserves agreement with the reference data for radial positions outside the training set, improving the reliability of its prediction. However, even though the so-obtained wave-packet is reliable in the near-field pressure prediction, this method cannot be useful to accurately predict the acoustic far-field probably due to the limitation of the training domain which included only near-field data, sometimes partially immersed in the jet flow.

To bypass the mentioned issue, this paper extends the findings put forth by Palma et al. [28], improving the model capabilities by integrating data from both near and far fields in the derivation of the wave-packet parameters via a multi-objective optimization.

The training data are derived from the same high-fidelity LES as in the work of Palma et al. [28]. However, this study enhances the predictive accuracy of the wave-packet model by introducing an additional objective function in the minimization process to refine the model performance in the far-field. Moreover, a tailored decision procedure to extract the optimal solution from the set resulting from the multi-objective optimization problem is proposed, leveraging the presence of the additional objective function. The problem is computed for various Strouhal numbers St, specifically focusing also in this paper on the 0^{th} azimuthal mode, which is highly representative of the energy content of the subsonic jet noise at the considered frequencies. The obtained wave-packets demonstrate utility in accurately predicting both near-field and far-field behaviors. Due to the accurate prediction both in the entire domain, and its fast evaluation, this wave-packet formulation is particularly well suited to be coupled with a wide range of aeroacoustic solvers, especially low and mid-fidelity methods.

The paper is organized as follows: the numerical setup that provided the data used in this work is briefly introduced in Section II. The wave-packet model and its optimization are described in Sections III and III.A, respectively. The results from the optimization are reported in Section IV. Final remarks can be found in Section V.

II. Numerical setup

The near-field of the isothermal round free jet at a Reynolds number $Re_D = 10^5$ used for this paper has been computed by LES. The nozzle exhaust jet Mach number has been fixed at $M = 0.9$, with the nozzle-exhaust boundary-layer thickness set at $\delta_{bl} = 0.15r_0$ and the nozzle exit turbulence intensity at 9% (see [29, 30] for details). The LES has been carried out using an in-house solver of the three-dimensional filtered compressible Navier-Stokes equations in cylindrical coordinates (r, θ, x) based on low-dissipation and low-dispersion explicit schemes. The quality of the grid for the present jet LES has been assessed in a previous work [31]. Specifically, the grid contains approximately one billion points. Pressure has been recorded at several locations spanning a large near-field domain and gaining time-resolved

signals, see reference [32] for a description of the available data. In addition, the near-pressure field of this jet has been also investigated in [33]. It has been propagated to the far field in [30, 34] using an in-house OpenMP-based solver of the isentropic linearized Euler equations in cylindrical coordinates based on the same numerical methods as the LES.

Concerning the near-field domain, we consider arrays of virtual microphones parallel to the nozzle exhaust, containing 1024 probes covering a domain that spans between x=0 and x/D=20. The data have been stored at a sampling frequency corresponding to St = 12.8, with a total of 3221 time snapshots. A representative one is shown in Fig.1. In the far field, we consider a polar arc of virtual microphones centred at the nozzle exit, positioned at $R = 75D$, from 15 to 165 degrees relative to the jet direction, with a spacing of one degree.

The original pressure signals are represented in terms of their azimuthal components through the azimuthal decomposition [35]. The Fourier coefficients are stored for the first four azimuthal modes that dominate the sound field for low polar angles. As aforementioned, the wave-packet model presented in this paper has been carried out for the 0^{th} azimuthal mode, which is dominant for the noise generation at Strouhal numbers lower than 1 [21].

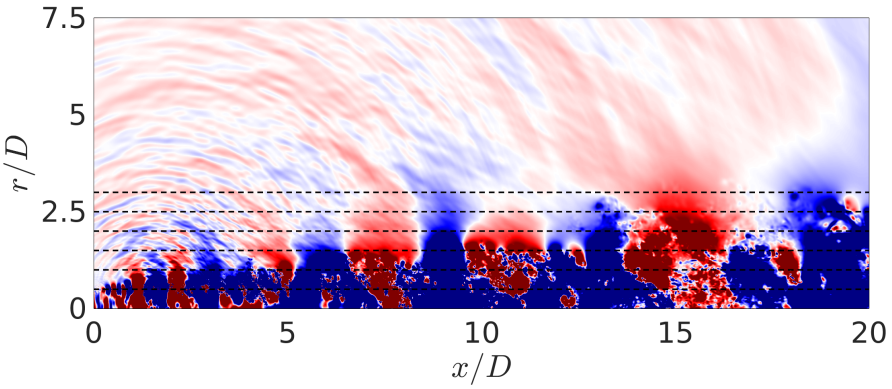

Fig. 1 Snapshot in the (x,r) plane of the pressure fluctuations. The black dashed lines represent the probe arrays in the near field.

III. Wave-packet model

A wave-packet model is used as a source for reproducing the noise produced by a subsonic jet. It has been introduced by Morris [36, 37], Tam and Burton [38], Crighton and Huerre [39], and Avital *et al.* [40]. The formulation adopted in this paper was derived by Papamoschou and coworkers [22, 25–27]. The model is based on the fundamental assumption stating that the peak noise radiation from the jet in the aft region is related to the large-scale coherent structures in the jet flow which can be modeled as instability waves at their boundaries, growing and then decaying along the axial distance [25].

The present formulation introduces a cylindrical virtual surface at a radial distance r_0 from the jet axis. The surface radiates the pressure perturbation imposed on it, representing and substituting the jet from the acoustic point of view. Applying the wave-packet ansatz, the pressure on the cylindrical surface surrounding the jet is prescribed as:

$$p_w(m, r_0, x, \theta, t) = p_0(x) e^{-i\omega t + im\phi}, \tag{1}$$

where m is the azimuthal mode number, x denotes the axial coordinate, ϕ is the azimuthal angle, $\omega = 2\pi f$ is the pulsation. The wave-packet axial shape $p_0(x)$ is given in the form [25]:

$$p_0(x) = \tanh\left(\frac{(x - x_0)^{p_1}}{b_1^{p_1}}\right)\left[1 - \tanh\left(\frac{(x - x_0)^{p_2}}{b_2^{p_2}}\right)\right] e^{i\alpha(x - x_0)}. \tag{2}$$

The radial distance of the virtual surface is taken as $r_0 = D/2$. The coordinate x_0 is used to locate the relative position between the origin of the wave-packet function and the nozzle exit. The two are considered to be coincident in this work, *i.e.*, $x_0 = 0$. The signal growth is controlled by the parameters b_1 and p_1, while b_2 and p_2 define its decaying rate. Following Morris [37], and Papamoschou [25], the solution in the linear regime (*i.e.*, solution for the 3D wave equation in cylindrical polar coordinates) for an arbitrary radial distance $r \geq r_0$ can be evaluated as

$$\begin{aligned} p_w(m, r, x, \theta, t) &= \frac{1}{2\pi} e^{-i\omega t + im\phi} \int_{-\infty}^{\infty} \hat{p}_0(k) \frac{H_m^{(1)}(\lambda r)}{H_m^{(1)}(\lambda r_0)} e^{ikx} dk \\ \text{with} \quad \lambda &= \left[\left(\frac{\omega}{c_\infty}\right)^2 - k^2\right]^{1/2}, \qquad -\frac{\pi}{2} < arg(\lambda) < \frac{\pi}{2}, \end{aligned} \tag{3}$$

where $\hat{p}_0(k)$ is the Fourier transform of $p_0(x)$, c_∞ is the speed of sound of the unperturbed flow, and $H_m^{(1)}$ is the Hankel function of the first kind and order m. In the radiation process, particular care must be taken to the spatial length of the wave-packet from the numerical point of view. A premature truncation of the waveform introduces noise and errors in the signal propagated to higher r. The phase speed can be used to distinguish among the radiative and non-radiative components of the pressure field generated by the wave-packet, characterized respectively by supersonic ($|\omega/k| \geq c_\infty$) and subsonic ($|\omega/k| < c_\infty$) values.

A. Wave-packet optimization

In this work, the method described in Palma et al. [28] is followed and further extended. The wave-packet noise source introduces some parameters whose value can be adjusted to match the pressure fluctuations from the reference jet using LES. A wave-packet describing the pressure fluctuations for a free jet is obtained by optimizing its parameters with near-field data on co-axial lines at two radial distances from the jet axis, namely $r/D = 2$ and 2.5, and on a far-field polar arc, $R = 75D$. The radial distance of the near field probes has been chosen considering that the wavepacket model

is valid for lines that are outside of the jet stream, and at the same time sufficiently close to the jet to sense and provide information about the hydrodynamic component of the pressure fluctuation. The near field reference data are obtained through LES simulation [30, 41] and the acoustic perturbations have been propagated to the far-field using a solver of the isentropic linearized Euler equations in cylindrical coordinates [30, 34] based on the same numerical methods as the LES, as described in Section II. In the following, the data at the mentioned lines and arc are referred to as *training* set, meaning that the model is informed by these data, while a *test* set is composed of the pressure field at other monitoring points.

The training of the model is performed using a multi-objective optimization procedure. The unconstrained optimization problem consists of the research of the set of variables $\mathbf{v}$ that yields a minimum of the N_J objective functions $J_n(\mathbf{v}, \mathbf{q})$

$$\begin{aligned} &\text{minimize } [J_n(\mathbf{v}, \mathbf{q})], \qquad n = 1, ..., N_J \text{ and } \mathbf{v} \in \mathcal{D}_\mathbf{v} \\ &\text{with bounds } v_s^L \leq v_s \leq v_s^U, \qquad s = 1, ..., N_v \end{aligned} \tag{4}$$

where $\mathbf{q}$ is the vector of the fixed parameters, $\mathbf{v}$ is the vector of the N_v design variables bounded by v_n^L and v_n^U in the design space $\mathcal{D}_\mathbf{v}$. In the present application, $\mathbf{v}$ represents the vector collecting the wave-packet parameters $\mathbf{v} = \left[p_1, b_1, p_2, b_2, \omega/(\alpha U_j)\right]$, while the vector $\mathbf{q}$ contains, among the others, the azimuthal order $m = 0$, the St number, the speed of sound of the unperturbed flow c_∞, etc. Suitable boundaries are selected for the components of $\mathbf{v}$, as reported in Table 1. The number of objective functions to be minimized at the same time is $N_j = 3$ and are described by

Table 1 Lower and upper bounds of optimization variables.

	p_1	b_1	p_2	b_2	$\omega/(\alpha U_j)$
min	0.2	0.022	1.2	0.022	0.43
max	40	0.44	40	0.44	0.75

$$J_n(\mathbf{x}, \mathbf{y}) = \sqrt{\int_{\mathcal{L}_n} \left(\frac{|p_n - \hat{p}_{REF_n}|}{\max\left(|\hat{p}_{REF_n}|\right)} \right)^2 ds} \tag{5}$$

where $\hat{p}_{REF_n} = p_{REF_n}/\hat{p}$ is the value of the reference pressure field on the n-th line, numerically evaluated by LES or LEE simulations, normalized with $\hat{p}$ the maximum value at the line $r/D = 0.5$. The objective functions represent the L2-norm of the difference between the pressure predicted by the wave-packet source model and the reference pressure from the numerical simulations, namely LES in the near field for $n = 1, 2$ and LEE for the far field arc for $n = 3$. The integral in Eq. (5) is defined over the axial extension from 0 up to $x/D = 20$ for the lines in the near field, $(r_n = 2D, 2.5D)$, defining J_1 and J_2. For the definition of J_3, the integral extends over a polar arc, ranging from 15 to 165 degrees, centered on the jet axis at the nozzle exit with radius $R = 75D$. According to Eq. 5, each objective function

is normalized by the peak value from the reference pressure field on the respective line $\mathcal{L}_n$. Both the hydrodynamic and the acoustic parts of the pressure fluctuations are included in the p_{REF}, hence the resulting wavepacket is expected to reproduce the complete fluctuation envelope, with the limitation given by the hypothesis that the wave-packet is not immersed in the jet flow. The optimizations are performed using a Multi-Objective Particle Swarm Optimization algorithm [42, 43], using a fixed budget of 70 particles per variable (a total of 420) and 500 iterations.

IV. Results

When the objectives to be minimized are, at least partially, conflicting, the solutions of the optimization problems are such that it is not possible to find other points in the domain improving the score of one objective function without worsening the performance of at least one of the remaining ones. The solutions of a non-trivial multi-objective optimization are, hence, optimal in a Paretian sense [44], leading to the definition of non-dominated solutions, which form the approximated Pareto front of the optimization problem.

Figure 2 shows the non-dominated solutions obtained for the four considered *St* numbers at the end of the optimization procedures. The wave-packet parameters of the selected solutions are reported in Table 2. It is important to notice that all the solutions on the Pareto fronts have the same dignity and the preferred one can be chosen at will by the designer for the problem at hand [45]. A ranking criterion can be identified to help the decision process, which can be arbitrarily defined: from simple subjective preferences to more complex analyses of the results are in principle all valid methods to pick only one of the Pareto optimal solutions [46–48].

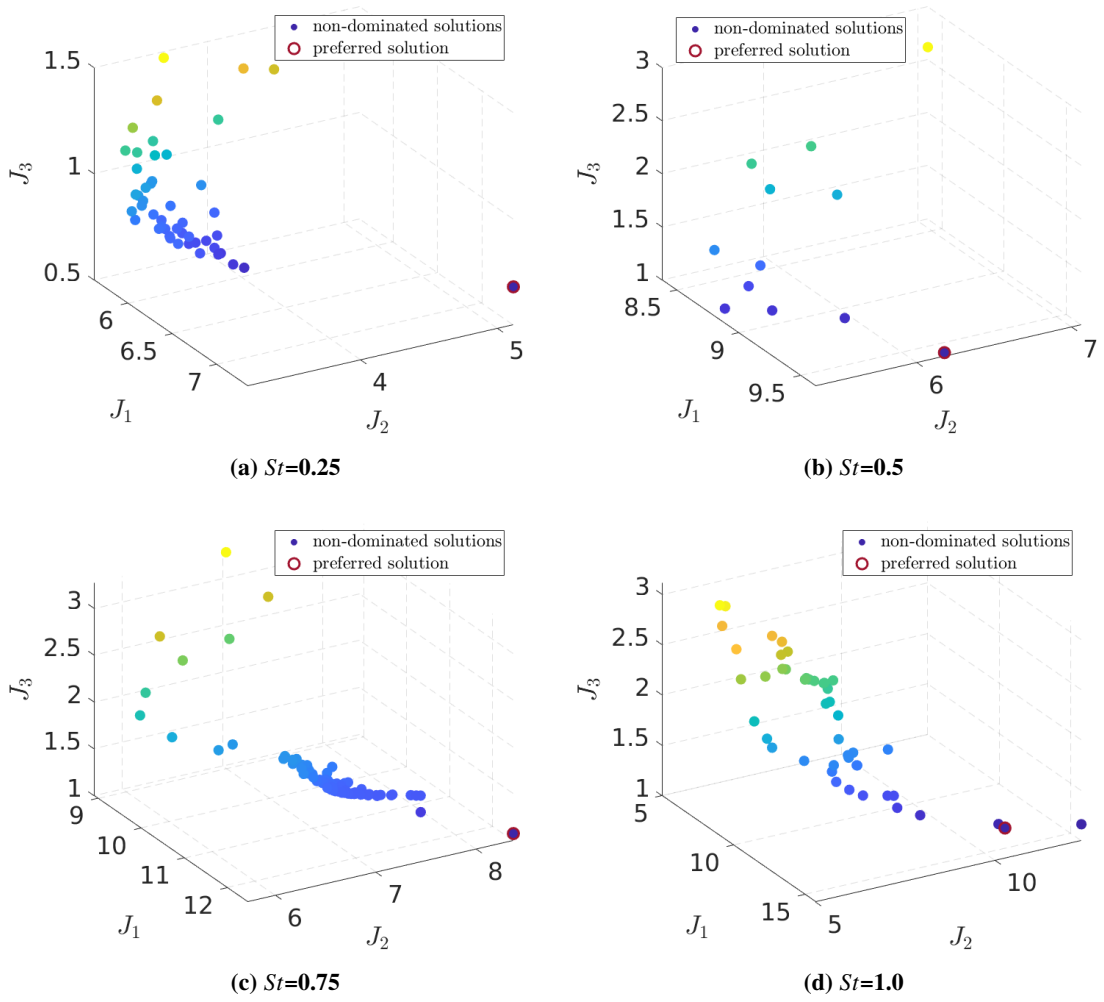

(a) St**=0.25** **(b)** St**=0.5**

(c) St**=0.75** **(d)** St**=1.0**

Fig. 2 Solutions of the optimization problems for the considered St numbers. Points are colored with the value of the ranking criterion, from blue to yellow.

In this study, one of the already evaluated objective functions is used as the ranking criterion: the solutions are ordered by their J_3 result, and the one minimizing the reproduction error on the far field line is taken as the preferred solution. The mentioned choice is justified by the fact that the integration lines $\mathcal{L}_n$ ($n \in]1,2[$) in the near field objectives functions are partially immersed in the jet flow. In Fig. 3, a rough estimation of the portions of the lines immersed in the jet stream is obtained assuming a spreading angle for the jet of 7° [49]. Reference data are noted to have high-frequency oscillations at axial positions that are estimated to be in-flow.

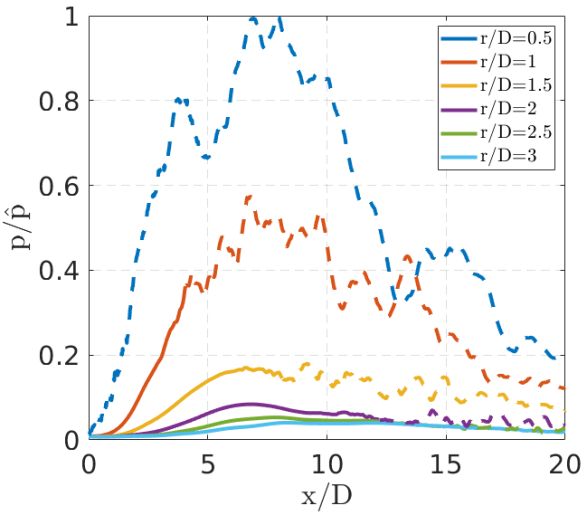

Fig. 3 Reference field from LES on near field axial lines at several r/D. Dashed lines refer to the portion of data that are estimated to be immersed in the jet, assuming a 7° opening angle.

As it has been stated in Section III, the model assumes the monitoring points to be outside the jet stream. Hence, the solutions that try to tightly follow the p_{REF} of the near field lines may be driven away from the "correct" wavepacket shape by the influence of the jet flow in the reference pressure field. Therefore, it is reasonable to assume that the evaluation of J_1 and J_2 is affected by some error when calculating the difference between the predicted and simulated pressure for large axial positions, even for the "correct" wave-packet. It is important to stress that the use of the multi-objective optimization with near- and far-field data, and the subsequent selection of the preferred solution by means of the presented ranking criterion is absolutely not equivalent to the optimization of the wavepacket using only far-field data. In fact, any solution to the multi-objective problem has been obtained simultaneously minimizing the objective functions related to both the near-field and far-field predictions. It can be said that the preferred solution is the best far-field solution that at the same time optimizes the near-field response.

To get noise prediction for a wide range of frequencies a dedicated optimization is performed for each of the considered St numbers, namely 0.25, 0.5, 0.75, and 1.

Figures 4 to 7 show the comparison between the reference pressure field and the one predicted by the optimal wave-packets at six near-field radial distances and the far-field polar arc, for the four mentioned St numbers. It is important to stress that, among the near-field axial lines on which the results are presented, only data from radial distances $r/D = 2$ and 2.5 were used in the optimization as a "training set". The other distances can be interpreted as a "test set" for the wave-packets. As evidenced by comparing the aforementioned figures, for higher St the optimization struggles a bit more in finding a wavepacket whose solution well reproduces the near field. It is interesting to note that the selected solutions closely reproduce the shape of the reference data on the near field lines only up to roughly the axial position where the lines start to be inside the jet flow for all the considered St (being the $r/D = 0.5$ line completely

immersed, the wave-packet prediction over that line is typically off compared with the reference pressure). The test lines confirm that the optimized wave-packets catch the characteristics of the jet noise source, correctly capturing the radial decaying of the pressure fluctuations deriving from the relative importance of the hydrodynamic and acoustic part of the wavepacket source. The effect of the St on the reproduction on the far field is limited by the ranking criterion used to select the preferred solution.

The optimized solutions show an excellent capability of capturing the emission peak from the jet for all the studied St, see Fig. 4-7(g), while appearing to lack energy for polar angles larger than 100°. This is reflected also in Fig. 8, where the comparison between the frequency spectrum of the reference signal in the far-field and the one obtained with the optimized wave-packets is shown around the maximum directivity angle, $\theta = 40°$, in a direction normal to the jet axis and aligned with the nozzle exit, $\theta = 90°$, and for a large polar angle pointing rearward, $\theta = 130°$. This can be ascribed to the characteristics of the wave-packet source, which is able to model the sound emission by large-scale turbulent structures in the jet, that dominate in the downstream direction (see Cavalieri et al. [21], Morris [37], Tam et al. [50]). However, the wave-packet source has a limited emission at large polar angles, where the radiated noise mainly comes from fine-scale turbulent motions. This results in an underprediction of upstream traveling waves. To improve prediction accuracy at higher polar angles, given the limitations of the wave-packet approach, a potential future step involves combining the presented model with a localized omnidirectional noise source near the nozzle exit [25]. This source can be generated considering an acoustic monopole or higher-order modes, such as the helical mode (m=1) and the double-helical mode (m=2)[18], since these modes play a more significant role in the sideline direction [51].

Wave-packets with very different shapes and parameters can be found in the Pareto front of each optimization, obtaining a similar result on the ranking criterion, *i.e.* on the far-field prediction. However, their performance on the near-field is completely different. This confirms the ill-posedness of the inverse acoustic problem when the wave-packet is retrieved from far-field measures only, highlighting the importance of including both near and far-field lines in the optimization procedure.

Table 2 Wave-packet parameters of the selected optimal solutions.

St	p_1	b_1	p_2	b_2	$\omega/(\alpha U_j)$
0.25	3.988	0.1224	8.366	0.2029	0.725
0.50	14.221	0.1093	14.559	0.1636	0.531
0.75	20	0.0914	12.929	0.1283	0.570
1.0	37.704	0.0995	26.041	0.1450	0.550

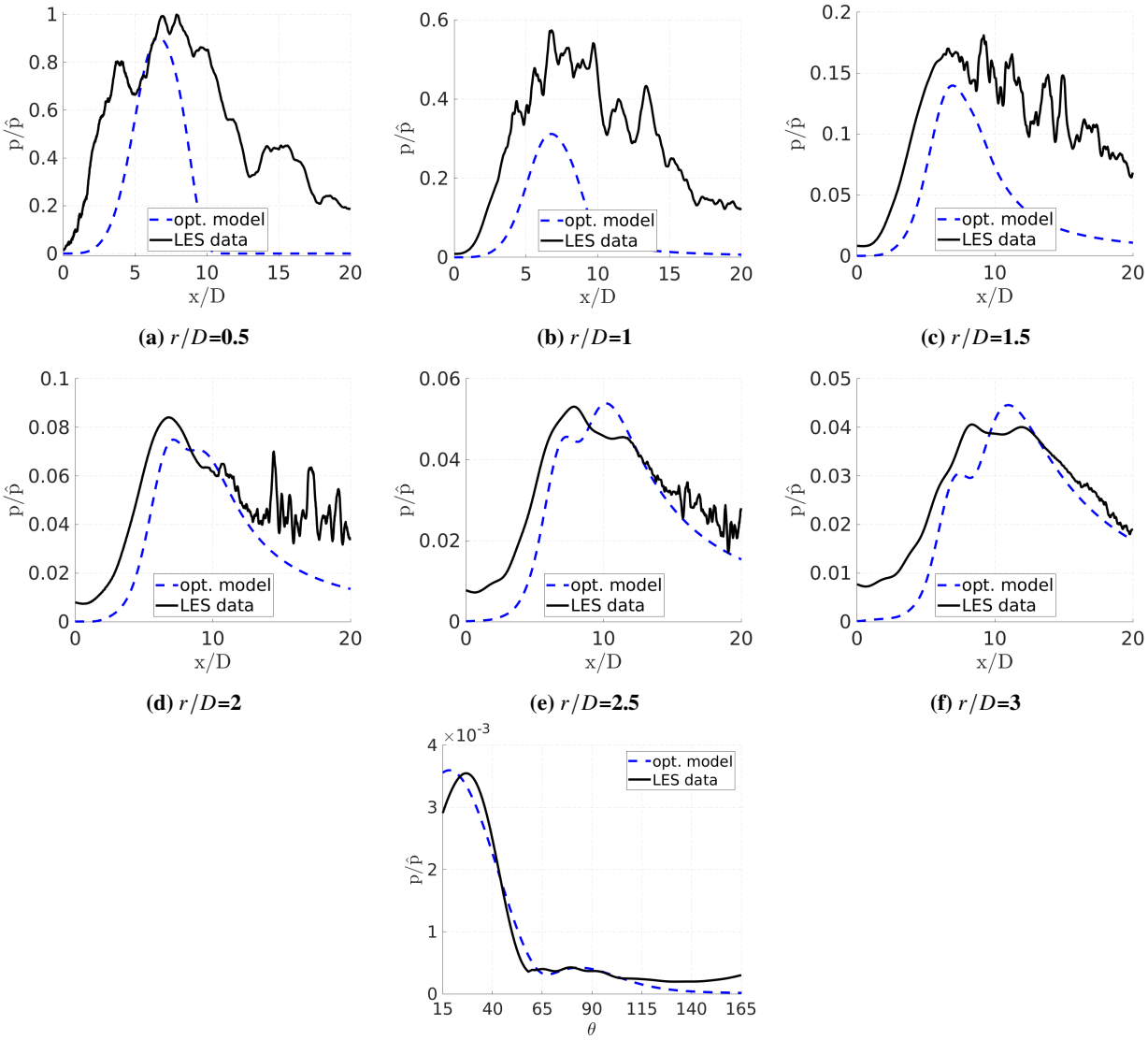

(a) r/D**=0.5** **(b)** r/D**=1** **(c)** r/D**=1.5**

(d) r/D**=2** **(e)** r/D**=2.5** **(f)** r/D**=3**

(g) R**=75D**

Fig. 4 Comparison between reference and optimized wave-packet normalized pressure. Near-field predictions in figures from (a) to (f), far-field prediction in (g), $St = 0.25$**.**

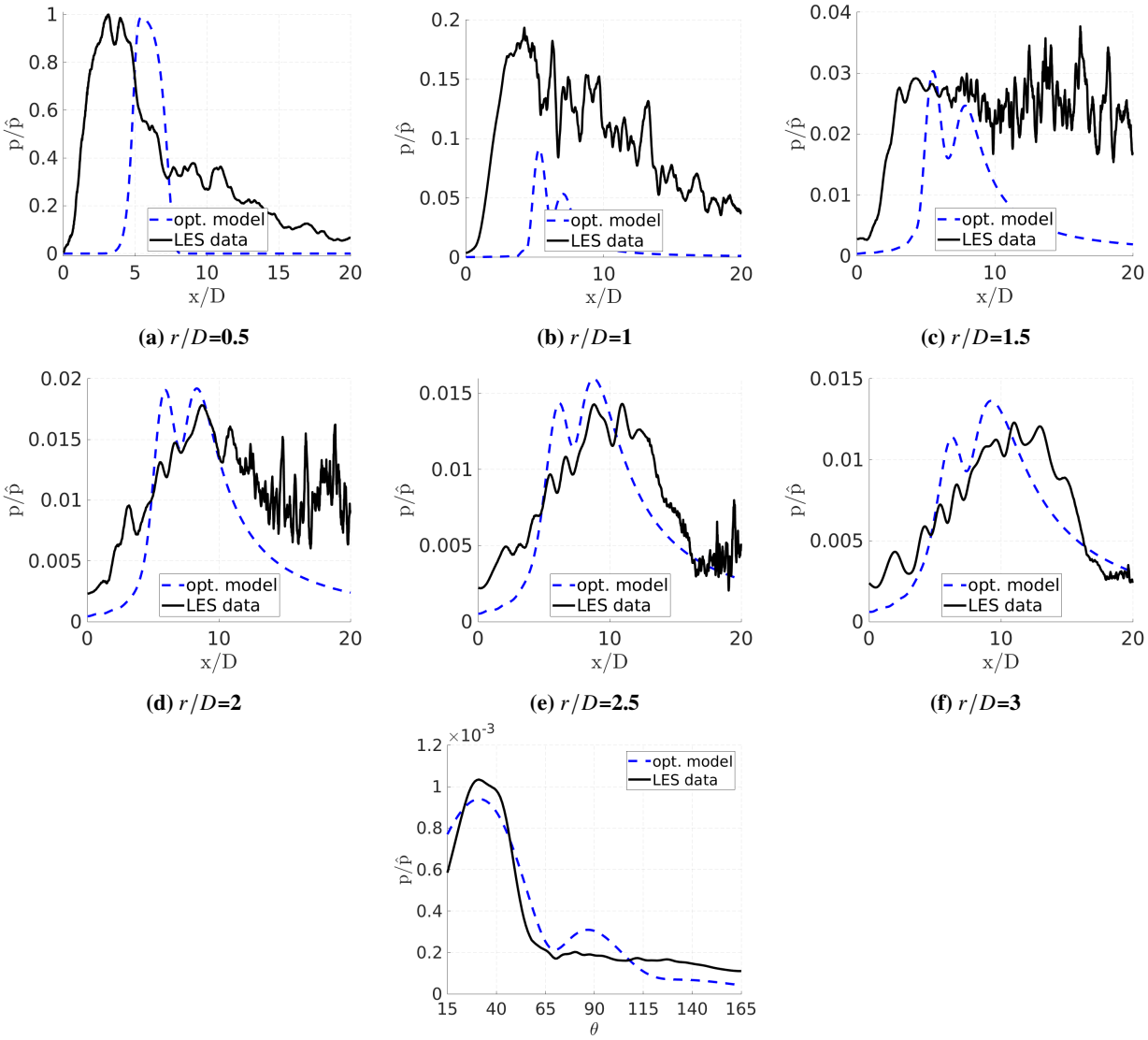

(a) r/D**=0.5** **(b)** r/D**=1** **(c)** r/D**=1.5**

(d) r/D**=2** **(e)** r/D**=2.5** **(f)** r/D**=3**

(g) R**=75D**

Fig. 5 Comparison between reference and optimized wave-packet normalized pressure. Near-field predictions in figures from (a) to (f), far-field prediction in (g), $St = 0.5$**.**

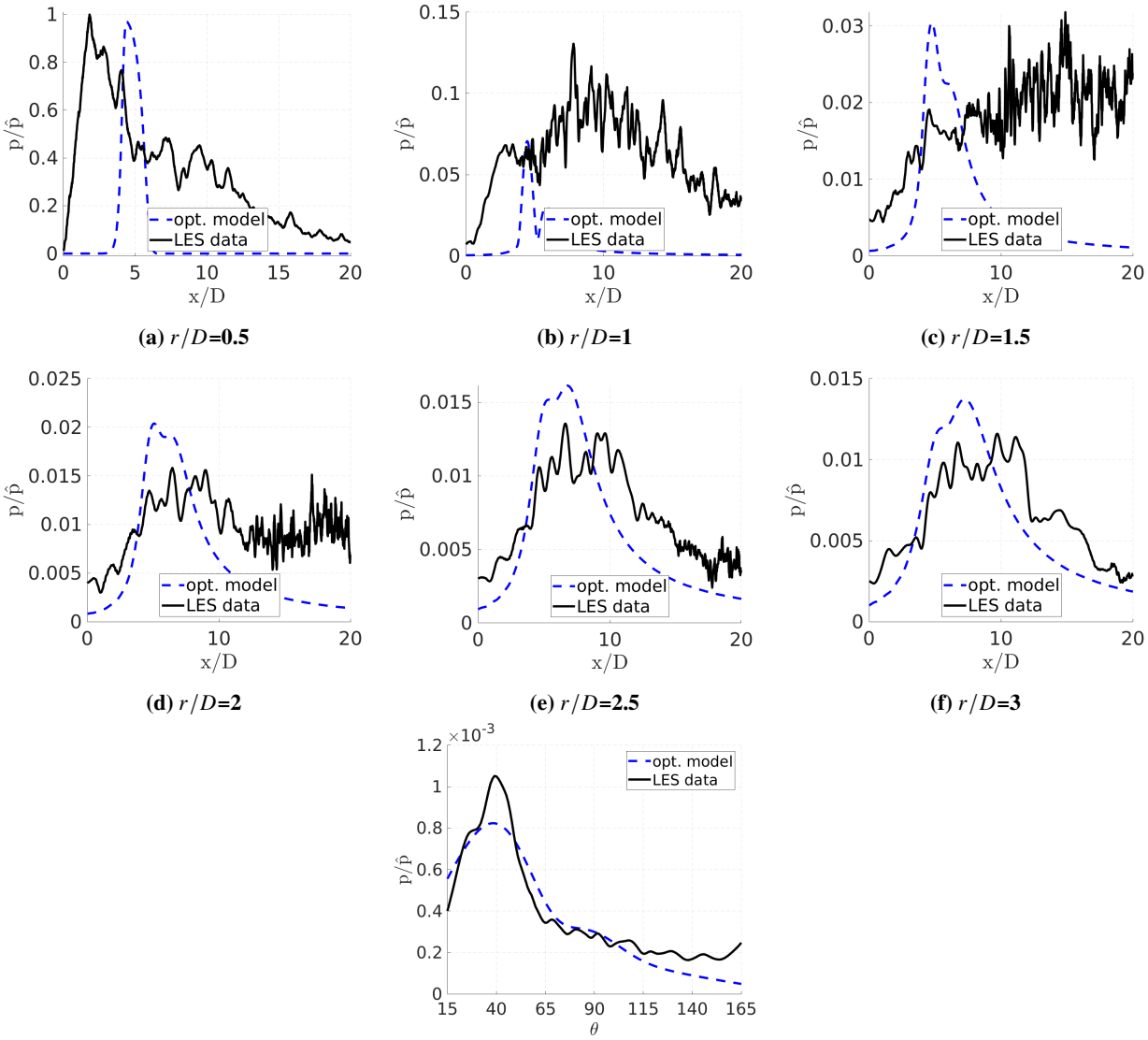

(a) r/D**=0.5** **(b)** r/D**=1** **(c)** r/D**=1.5**

(d) r/D**=2** **(e)** r/D**=2.5** **(f)** r/D**=3**

(g) R**=75D**

Fig. 6 Comparison between reference and optimized wave-packet normalized pressure. Near-field predictions in figures from (a) to (f), far-field prediction in (g), $St = 0.75$**.**

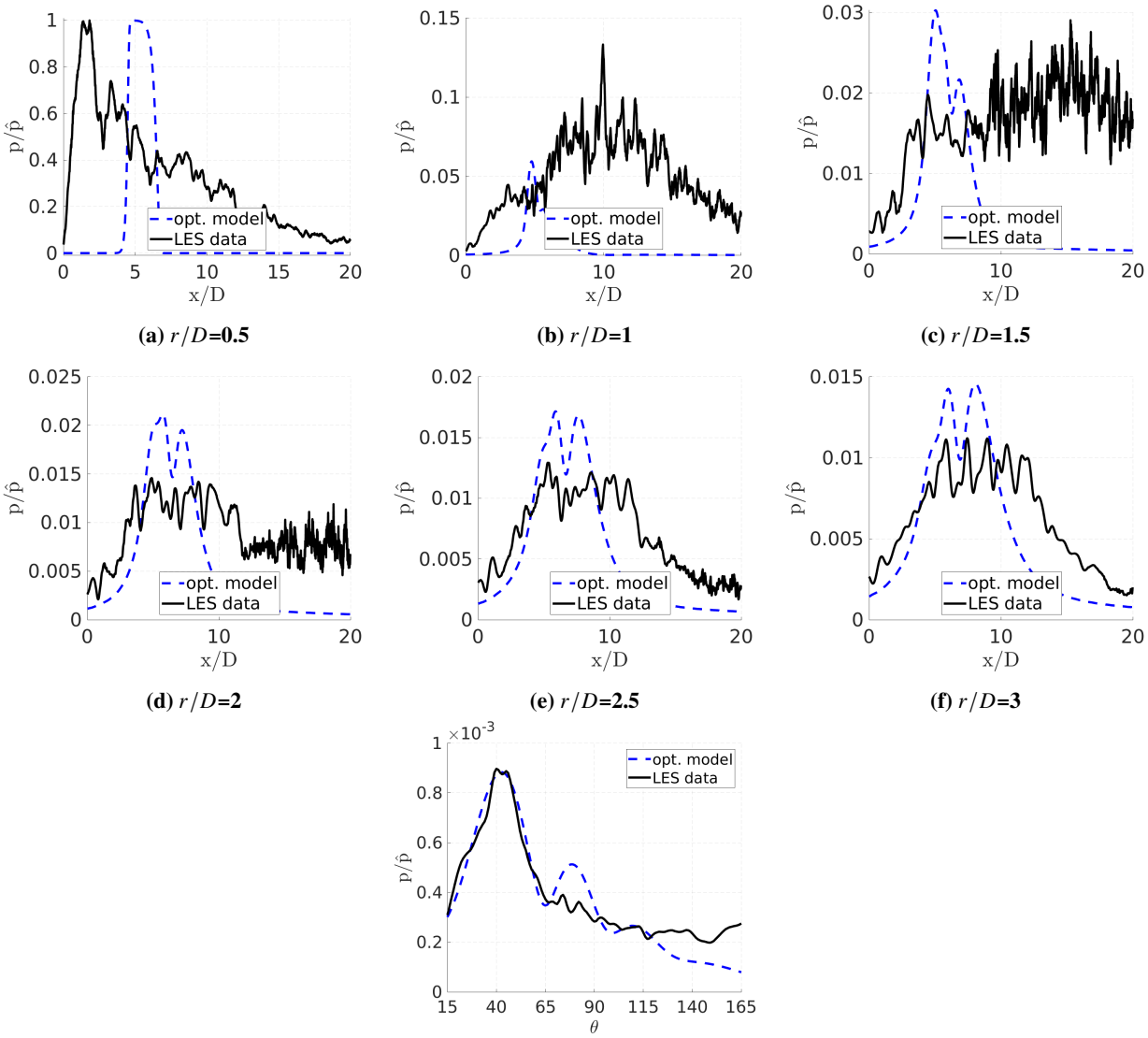

(a) r/D**=0.5** **(b)** r/D**=1** **(c)** r/D**=1.5**

(d) r/D**=2** **(e)** r/D**=2.5** **(f)** r/D**=3**

(g) R**=75D**

Fig. 7 Comparison between reference and optimized wave-packet normalized pressure. Near-field predictions in figures from (a) to (f), far-field prediction in (g), $St = 1.0$**.**

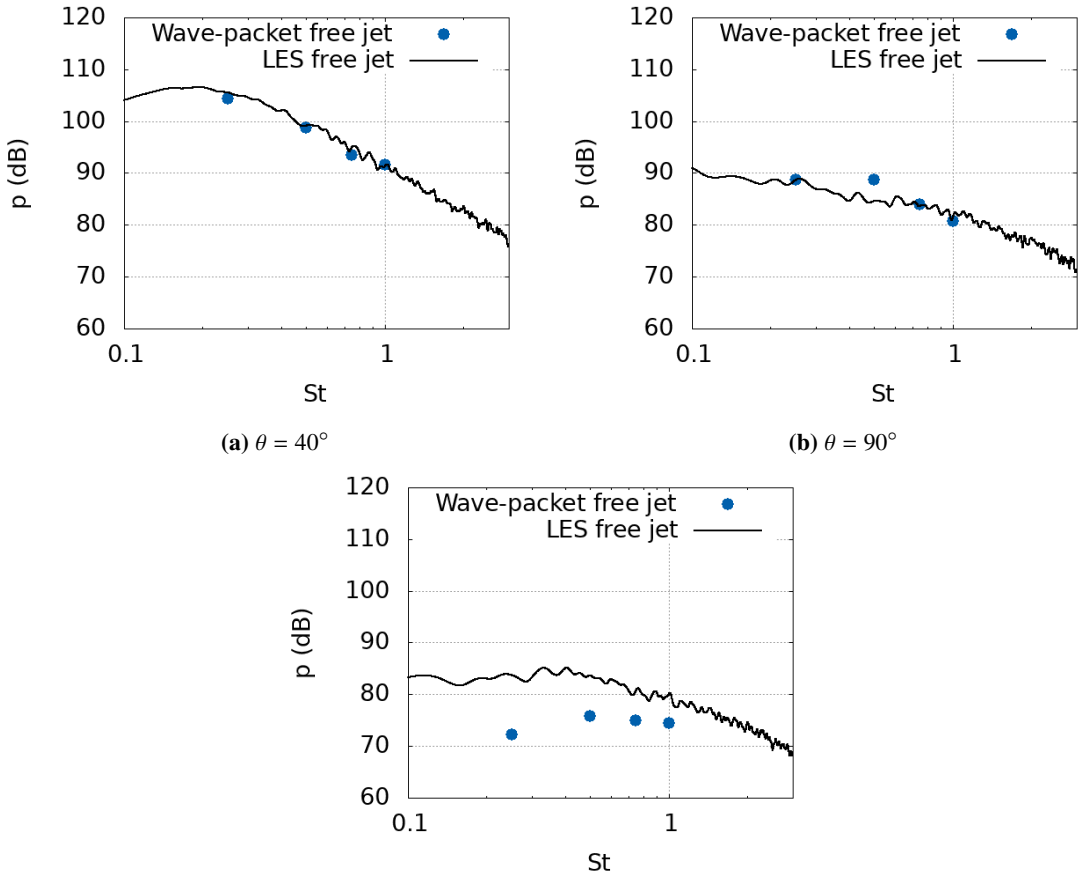

(a) $\theta = 40°$

(b) $\theta = 90°$

(c) $\theta = 130°$

Fig. 8 Far field noise spectra for $\theta = 40, 90, 130$ degrees

The analysis and optimization have been conducted here using data from a jet stream at $M = 0.9$. The calibration obtained can be reused for different Mach numbers: according to the literature [50], the shapes of the spectra should not change in the subsonic regime by reducing the jet Mach number. Energy spectra can, thus, be scaled by using empirical models available in the literature [52], and so the prediction from the wave-packets.

The methodology has been here applied to an axisymmetric jet, using only the m=0 azimuthal mode extracted from the LES data to optimize the wavepacket. According to the literature [53, 54], for a nozzle with chevrons, the acoustic far field is still associated mainly with the m=0 azimuthal mode, which remains the most efficient acoustically radiating mode for low polar angles. In other words, the acoustic field can still be accurately described by the 0-th azimuthal mode because the higher-order ones, whose order is related to the number of chevrons, are less acoustically efficient and do not significantly contribute to the emitted noise. The chevrons may be able to reduce the growth rate of the instabilities and increase the phase speeds of the waves compared to thrust-equivalent round jets. These effects are associated with their ability to reduce the radiation efficiency of large-scale structures and thus noise reductions. Consequently, the wave-packet must be calibrated on data from chevron jets to capture this phenomenon.

The proposed method can in principle be extended to account for some flight effects getting closer to realistic configurations of aeronautical interest. The effect on the acoustic propagation of a uniform free stream velocity can be included in the wave-packet model using the Prandtl-Glauert(PG) coordinate transformation [55]. In this way, the pressure field predicted by the wave-packet model can be corrected including the effects of a relative uniform motion between the nozzle/jet and the hosting fluid, under the hypothesis of irrotational perturbations propagating within a uniform mean flow. However, this correction cannot account for the influence of the flight stream on the jet characteristics, like the modification of the jet shape such as a shear layer or potential core length. To consider these effects related to a more realistic non-uniform flow, dedicated simulations or experiments must be conducted to produce a reliable training set for wave-packet calibration.

V. Conclusion

This study used a multi-objective optimization approach to identify the optimal parameters of a wave-packet model for jet flow noise prediction. A ranking criterion based on the agreement on far-field data was proposed to identify a unique solution among the Pareto front obtained from the optimizations. The preferred solution is not merely the best far-field solution as resulting from a single objective optimization, as the multi-objective approach simultaneously takes into consideration the near-field result in the error minimization process. The use of combined near- and far-field data is proved to be a robust method for guiding the optimization to solutions able to effectively predict both the hydrodynamic and the acoustic component of the pressure fluctuations in the reference data. The optimized wave-packets show a notable capability of reproducing the pressure fluctuations in the whole domain. In particular, in the far-field, the directivity peak of the jet noise source is correctly captured and the noise spectra show a nice agreement up to polar angles of 90°. At higher angles, where the emitted noise is minimum, the modeled spectrum is underpredicted, especially for lower frequencies. The fast evaluation and accuracy of the model in both the near and far field make it well suited to be coupled with low and mid-fidelity aeroacoustic solvers (such as BEM solvers) for jet noise scattering predictions, with the simplifying hypothesis that the acoustic field can be effectively separated into an incident and a scattering part. This means that the jet aerodynamics/shape can be considered not to be strongly influenced by the presence of the scattering surfaces (*i.e.,* the acoustic source is independent of its position), and thus the pressure field produced by the wave-packet model can be used as the incident field in a scattering code.

Acknowledgments

C. Bogey was partially supported by the LABEX CeLyA (ANR-10-LABX-0060/ANR-16-IDEX-0005). The numerical data analyzed in this work were obtained using the HPC resources of PMCS2I (Pôle de Modélisation et de Calcul en Sciences de l'Ingénieur et de l'Information) of Ecole Centrale de Lyon, and the resources of IDRIS (Institut du Développement et des Ressources en Informatique Scientifique) under the allocation 2021-2a0204 made by GENCI

(Grand Equipement National de Calcul Intensif).

References

[1] Baudin, C., Lefèvre, M., Champelovier, P., Lambert, J., Laumon, B., and Evrard, A.-S., "Aircraft Noise and Psychological Ill-Health: The Results of a Cross-Sectional Study in France," *International Journal of Environmental Research and Public Health*, Vol. 15, No. 8, 2018. https://doi.org/10.3390/ijerph15081642.

[2] Basner, M., and McGuire, S., "WHO Environmental Noise Guidelines for the European Region: A Systematic Review on Environmental Noise and Effects on Sleep," *International Journal of Environmental Research and Public Health*, Vol. 15, No. 3, 2018. https://doi.org/10.3390/ijerph15030519.

[3] "Global trends in aircraft noise," , 2022. URL https://www.icao.int/environmental-protection/Pages/Noise_Trends.aspx.

[4] Burghignoli, L., Di Marco, A., Centracchio, F., Camussi, R., Ahlefeldt, T., Henning, A., Adden, S., and Di Giulio, M., "Evaluation of the noise impact of flap-tip fences installed on laminar wings," *CEAS Aeronautical Journal*, Vol. 11, No. 4, 2020, pp. 849–872. https://doi.org/10.1007/s13272-020-00454-x.

[5] Jawahar, H. K., Meloni, S., and Camussi, R., "Jet noise sources for chevron nozzles in under-expanded condition," *International Journal of Aeroacoustics*, Vol. 0, No. 0, 2022, pp. 1–16. https://doi.org/10.1177/1475472X221101766.

[6] Meloni, S., and Jawahar, H. K., "A Wavelet-Based Time-Frequency Analysis on the Supersonic Jet Noise Features with Chevrons," *Fluids*, Vol. 7, No. 3, 2022. https://doi.org/10.3390/fluids7030108.

[7] Iemma, U., and Palma, G., "Optimization of metasurfaces for the design of noise trapping metadevices," *Proceedings of the 26th International Congress on Sound and Vibration, ICSV 2019*, 2019.

[8] Palma, G., and Burghignoli, L., "On the integration of acoustic phase-gradient metasurfaces in aeronautics," *International Journal of Aeroacoustics*, Vol. 19, No. 6-8, 2020, pp. 294–309. https://doi.org/10.1177/1475472x20954404.

[9] Palma, G., Burghignoli, L., Centracchio, F., and Iemma, U., "Innovative Acoustic Treatments of Nacelle Intakes Based on Optimised Metamaterials," *Aerospace*, Vol. 8, No. 10, 2021. https://doi.org/10.3390/aerospace8100296.

[10] Jones, M. G., Nark, D. M., and Schiller, N. H., "Evaluation of Variable-Depth Liners with Slotted Cores," *28th AIAA/CEAS Aeroacoustics 2022 Conference*, 2022. https://doi.org/10.2514/6.2022-2823.

[11] Dodge, C., Howerton, B. M., and Jones, M. G., "An Acoustic Liner with a Multilayered Active Facesheet," *28th AIAA/CEAS Aeroacoustics 2022 Conference*, 2022. https://doi.org/10.2514/6.2022-2902.

[12] Palani, S., Murray, P., McAlpine, A., Knepper, K., and Richter, C., "Experimental and numerical assessment of novel acoustic liners for aero-engine applications," *28th AIAA/CEAS Aeroacoustics 2022 Conference*, 2022. https://doi.org/10.2514/6.2022-2900.

[13] Palma, G., Centracchio, F., and Burghignoli, L., "Optimized metamaterials for enhanced noise shielding of innovative aircraft configurations," Silesian University Press, 2021. URL https://www.scopus.com/inward/record.uri?eid=2-s2.0-85117392599&partnerID=40&md5=10c0b4357215b5c49141639735dd57ce.

[14] Liebeck, R. H., "Design of the Blended Wing Body Subsonic Transport," *Journal of Aircraft*, Vol. 41, No. 1, 2004, pp. 10–25. https://doi.org/10.2514/1.9084.

[15] Centracchio, F., Burghignoli, L., Rossetti, M., and Iemma, U., "Noise shielding models for the conceptual design of unconventional aircraft," *INTER-NOISE 2018 - 47th International Congress and Exposition on Noise Control Engineering: Impact of Noise Control Engineering*, 2018.

[16] Burghignoli, L., Centracchio, F., Iemma, U., and Rossetti, M., "Multi-objective optimization of BWB aircraft for noise shielding improvement," *25th International Congress on Sound and Vibration 2018, ICSV 2018: Hiroshima Calling*, Vol. 2, International Institute of Acoustics and Vibration, IIAV, 2018, p. 1256 – 1263.

[17] Xie, J., Cai, Y., Chen, M., and Mavris, D. N., "Integrated Sizing and Optimization of Hybrid Wing Body Aircraft in Conceptual Design," *AIAA Aviation 2019 Forum*, 2019. https://doi.org/10.2514/6.2019-2885.

[18] Papamoschou, D., and Mayoral, S., "Jet noise shielding for advanced hybrid wing-body configuration," *49th AIAA Aerospace Sciences Meeting including the New Horizons Forum and Aerospace Exposition*, 2011, p. 912.

[19] Denisov, S., and Korolkov, A., "Investigation of noise-shielding efficiency with the method of sequences of maximum length in application to the problems of aviation acoustics," *Acoustical Physics*, Vol. 63, No. 4, 2017, pp. 462–477.

[20] Lighthill, M. J., and Newman, M. H. A., "On sound generated aerodynamically I. General theory," *Proceedings of the Royal Society of London. Series A. Mathematical and Physical Sciences*, Vol. 211, No. 1107, 1952, pp. 564–587. https://doi.org/10.1098/rspa.1952.0060.

[21] Cavalieri, A. V. G., Jordan, P., Colonius, T., and Gervais, Y., "Axisymmetric superdirectivity in subsonic jets," *Journal of Fluid Mechanics*, Vol. 704, 2012, p. 388–420. https://doi.org/10.1017/jfm.2012.247.

[22] Huang, C., and Papamoschou, D., "Numerical Study of Noise Shielding by Airframe Structures," *14th AIAA/CEAS Aeroacoustics Conference (29th AIAA Aeroacoustics Conference)*, 2008. https://doi.org/10.2514/6.2008-2999.

[23] Towne, A., Cavalieri, A. V. G., Jordan, P., Colonius, T., Schmidt, O., Jaunet, V., and Brès, G. A., "Acoustic resonance in the potential core of subsonic jets," *Journal of Fluid Mechanics*, Vol. 825, 2017, p. 1113–1152. https://doi.org/10.1017/jfm.2017.346.

[24] Nogueira, P. A. S., Self, H. W. A., Towne, A., and Edgington-Mitchell, D., "Wave-packet modulation in shock-containing jets," *Phys. Rev. Fluids*, Vol. 7, 2022, p. 074608. https://doi.org/10.1103/PhysRevFluids.7.074608.

[25] Papamoschou, D., "Prediction of Jet Noise Shielding," *48th AIAA Aerospace Sciences Meeting Including the New Horizons Forum and Aerospace Exposition*, 2010. https://doi.org/10.2514/6.2010-653.

[26] Papamoschou, D., "Wavepacket Modeling of the Jet Noise Source," *17th AIAA/CEAS Aeroacoustics Conference (32nd AIAA Aeroacoustics Conference)*, 2011. https://doi.org/10.2514/6.2011-2835.

[27] Papamoschou, D., "Wavepacket modeling of the jet noise source," *International Journal of Aeroacoustics*, Vol. 17, No. 1-2, 2018, pp. 52–69. https://doi.org/10.1177/1475472X17743653.

[28] Palma, G., Meloni, S., Camussi, R., Iemma, U., and Bogey, C., "Data-Driven Multiobjective Optimization of Wave-Packets for Near-Field Subsonic Jet Noise," *AIAA Journal*, Vol. 61, No. 5, 2023, pp. 2179–2188. https://doi.org/10.2514/1.J062261.

[29] Bogey, C., Marsden, O., and Bailly, C., "Large-eddy simulation of the flow and acoustic fields of a Reynolds number 105 subsonic jet with tripped exit boundary layers," *Physics of Fluids*, Vol. 23, 2011, p. 035104. https://doi.org/doi.org/10.1063/1.3555634.

[30] Bogey, C., "Acoustic tones in the near-nozzle region of jets: characteristics and variations between Mach numbers 0.5 and 2," *Journal of Fluid Mechanics*, Vol. 921, 2021, p. A3. https://doi.org/10.1017/jfm.2021.426.

[31] Bogey, C., "Grid sensitivity of flow field and noise of high-Reynolds-number jets computed by large-eddy simulation," *International Journal of Aeroacoustics*, Vol. 17, 2018, pp. 399 – 424. https://doi.org/doi.org/10.1177/1475472X18778287.

[32] Bogey, C., "A database of flow and near pressure field signals obtained for subsonic and nearly ideally expanded supersonic free jets using large-eddy simulations," https://hal.archives-ouvertes.fr/hal-03626787, 2022.

[33] Adam, A., Papamoschou, D., and Bogey, C., "Imprint of Vortical Structures on the Near-Field Pressure of a Turbulent Jet," *AIAA Journal*, Vol. 60, No. 3, 2022, pp. 1578–1591. https://doi.org/10.2514/1.J061010.

[34] Bogey, C., "Tones in the acoustic far field of jets in the upstream direction," *AIAA J.*, Vol. 60, No. 4, 2022, pp. 2397–2406. https://doi.org/10.2514/1.J061013.

[35] Michalke, A., and Fuchs, H., "On turbulence and noise of an axisymmetric shear flow," *Journal of Fluid Mechanics*, Vol. 70, No. 1, 1975, pp. 179–205. https://doi.org/10.1017/S0022112075001966.

[36] Morris, P. J., "Jet noise prediction: Past, present and future," *Canadian Acoustics*, Vol. 35, No. 3, 2007, p. 16–22. URL https://jcaa.caa-aca.ca/index.php/jcaa/article/view/1883.

[37] Morris, P. J., "A Note on Noise Generation by Large Scale Turbulent Structures in Subsonic and Supersonic Jets," *International Journal of Aeroacoustics*, Vol. 8, No. 4, 2009, pp. 301–315. https://doi.org/10.1260/147547209787548921.

[38] Tam, C. K. W., and Burton, D. E., "Sound generated by instability waves of supersonic flows. Part 2. Axisymmetric jets," *Journal of Fluid Mechanics*, Vol. 138, 1984, p. 273–295. https://doi.org/10.1017/S0022112084000124.

[39] Crighton, D. G., and Huerre, P., "Shear-layer pressure fluctuations and superdirective acoustic sources," *Journal of Fluid Mechanics*, Vol. 220, 1990, p. 355–368. https://doi.org/10.1017/S0022112090003299.

[40] Avital, E. J., Sandham, N. D., and Luo, K. H., "Mach Wave Radiation by Mixing Layers. Part I: Analysis of the Sound Field," *Theoretical and Computational Fluid Dynamics*, Vol. 12, 1998, pp. 73–90. https://doi.org/doi.org/10.1007/s001620050100.

[41] Camussi, Roberto, Meloni, Stefano, and Bogey, Christophe, "On the influence of the nozzle exhaust initial conditions on the near field acoustic pressure," *Acta Acustica*, Vol. 6, 2022, p. 57. https://doi.org/10.1051/aacus/2022051.

[42] Coello, C., Pulido, G., and Lechuga, M., "Handling multiple objectives with particle swarm optimization," *IEEE Transactions on Evolutionary Computation*, Vol. 8, No. 3, 2004, pp. 256–279. https://doi.org/10.1109/TEVC.2004.826067.

[43] Sierra, M. R., and Coello Coello, C. A., "Improving PSO-Based Multi-objective Optimization Using Crowding, Mutation and $\in$-Dominance," *Evolutionary Multi-Criterion Optimization*, edited by C. A. Coello Coello, A. Hernández Aguirre, and E. Zitzler, Springer Berlin Heidelberg, Berlin, Heidelberg, 2005, pp. 505–519. https://doi.org/doi.org/10.1007/978-3-540-31880-4_35.

[44] Martins, J. R. R. A., and Ning, A., *Engineering Design Optimization*, Cambridge University Press, 2021. https://doi.org/10.1017/9781108980647.

[45] Bragge, J., Korhonen, P., Wallenius, H., and Wallenius, J., "Bibliometric Analysis of Multiple Criteria Decision Making/Multiattribute Utility Theory," *Multiple Criteria Decision Making for Sustainable Energy and Transportation Systems*, edited by M. Ehrgott, B. Naujoks, T. J. Stewart, and J. Wallenius, Springer Berlin Heidelberg, Berlin, Heidelberg, 2010, pp. 259–268.

[46] Iemma, U., Centracchio, F., and Burghignoli, L., "Aircraft sound quality as Pareto ranking criterion in multi-objective MDO," *INTER-NOISE and NOISE-CON Congress and Conference Proceedings*, Vol. 255, Institute of Noise Control Engineering, 2017, pp. 4946–4955.

[47] Zakeri, S., "Ranking based on optimal points multi-criteria decision-making method," *Grey Systems: Theory and Application*, 2018.

[48] Iemma, U., and Centracchio, F., "Sound-Quality-Based Decision Making in Multiobjective Optimisation of Operations for Sustainable Airport Scenarios," *Aerospace*, Vol. 9, No. 6, 2022. https://doi.org/10.3390/aerospace9060310.

[49] Bogey, C., Marsden, O., and Bailly, C., "Influence of initial turbulence level on the flow and sound fields of a subsonic jet at a diameter-based Reynolds number of 10^5," *Journal of Fluid Mechanics*, Vol. 701, 2012, p. 352–385. https://doi.org/10.1017/jfm.2012.162.

[50] Tam, C. K. W., Viswanathan, K., Ahuja, K. K., and Panda, J., "The sources of jet noise: experimental evidence," *Journal of Fluid Mechanics*, Vol. 615, 2008, p. 253–292. https://doi.org/10.1017/S0022112008003704.

[51] Nekkanti, A., and Schmidt, O. T., "Modal Analysis of Acoustic Directivity in Turbulent Jets," *AIAA Journal*, Vol. 59, No. 1, 2021, pp. 228–239. https://doi.org/10.2514/1.J059425.

[52] Zaman, K., and Yu, J., "Power spectral density of subsonic jet noise," *Journal of Sound and Vibration*, Vol. 98, No. 4, 1985, pp. 519–537. https://doi.org/https://doi.org/10.1016/0022-460X(85)90259-7.

[53] Gudmundsson, K., and Colonius, T., "Linear Stability Analysis of Chevron Jet Profiles," *Fluids Engineering Division Summer Meeting*, Vol. Volume 2: Fora, 2006, pp. 497–504. https://doi.org/10.1115/FEDSM2006-98485.

[54] Gudmundsson, K., and Colonius, T., "Spatial Stability Analysis of Chevron Jet Profiles," *13th AIAA/CEAS Aeroacoustics Conference (28th AIAA Aeroacoustics Conference)*, 2007. https://doi.org/10.2514/6.2007-3599.

[55] Rienstra, S., and Hirschberg, A., *An introduction to acoustics*, Technische Universiteit Eindhoven, 2004. Extended and revised edition of IWDE 92-06.